STUDIES OF FUNDAMENTAL PROCESSES IN HIGH POWER SWITCHES

M. A. Gundersen, W. Hartmann, G. Kirkman, and V. Dominic
University of Southern California
Los Angeles, California
90089-0484

The new high current switch discussed in this paper is a result of the study of the physics of high power switches. Optical diagnostics, including temporally and spatially resolved spectroscopy and quantitative models have been developed and applied, making it possible to understand physical processes that are responsible for the stability and current capability of the plasma. These methods and results are sufficiently general so that they should be applicable to the development of other plasma devices, including plasma accelerators and lenses. These results suggest that the study of basic physical processes is an important alternative approach to the development of new plasma devices.

INTRODUCTION

Increasing demands on the key elements of pulsed power devices, the switches, have led to the development of new types of high-power, low-pressure gas discharge switches: including the pseudo-spark /1-6/ and the BLT /7-9/ switch. Although these switches show several features combining the advantages of the thyratron and the pressurized spark gap, little is known about the physics involved. In particular, the extremely high current density at the initially cold cathode surface has not been explained. There is evidence for a more or less homogeneous current density distribution over an area of the order of $1cm^2$, resulting in an average current density of up to several 10 kA/cm^2 /9/. This is much greater than typical glow emission (~50-700 A/cm^2). These results and the attractive possibility of applications for a cathode with an order of magnitude increased emission provide compelling reasons for an investigation of the nature of the mechanism responsible for this extremely high cathode emissivity, and the influence of the discharge parameters on its occurrence.

The plasma device reported here is a result of a study of the fundamental processes occurring in high power gas discharge switches. The device is a hollow electrode superdense glow discharge that is initiated by light incident or the back of the cathode surface. The structure consists of two cup shaped electrodes each with a hole on axis (Fig. 1). It is filled with a low pressure ~0.1-0.5 of H_2, H_e or other inert gas. When charge carriers are added to the hollow space behind the cathode, an ionization avalanche occurs and forms a high current superdense glow discharge on axis. The cathode emission current density is very high due to a self heating of surface by ion bombardment during the avalanche phase of the discharge. The high axial current density ~$10kA/cm^2$ appears to be fairly uniform over an area of about 1 cm^2, resulting in a radial magnetic field linearly increasing with radius with a calculated gradient of ~10kG/cm. Presented here are results of an experimental study of this device directed towards understanding the fundamental processes important to high power discharge device development.

EXPERIMENT

Spectroscopic data were measured for the hydrogen Balmer alpha ($H\alpha$) and Balmer beta ($H\beta$) transitions in the plasma. These data are later used to estimate the electron temperature from the intensity ratio of $H\alpha$ to $H\beta$ at each point in space and time. The data also supplies electron density information via the $H\beta$ Stark broadening effect. Temporally and spatially resolved plasma intensity distributions for $H\alpha$ and $H\beta$ transitions were recorded by imaging the midplane of the discharge in the radial direction onto the entrance slit of a streak camera and using an appropriate analytical line filter. The imaged plane is parallel to the electrode faces and therefore contains radially symmetric intensity distributions. Subsequent Abel inversion of these distributions was performed to determine the true spatial intensity distribution for each of the transitions. To measure the Stark broadening of the $H\beta$ transition a similar set-up was used with the interference filter replaced by a 0.3 m spectrograph whose output at 485.5 nm was recorded with the streak camera. The streak data is therefore a picture of the linewidth as a function time. In this case, however, only one point in space may be observed at a time, and therefore the discharge must be scanned in the radial direction to obtain the desired spatial resolution. The spatial resolution in both cases was ≈2 mm in the axial as well as the radial direction.

The results presented here for both electron temperature and density are preliminary. They are limited by streak camera noise limitations, uncertainties in filter transmission and photocathode sensitivity, and the large number of data processing steps involved. They give, however, a rough estimation of the most essential plasma parameters and more importantly, their spatial and temporal behavior. We believe that they show with a reasonable accuracy the qualitative development of the plasma in space and time.

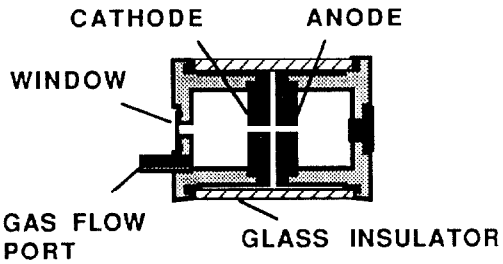

Figure (1). The experimental switch structure. The electrodes are cylindrically symetric each with a central hole of 5mm diameter and separated by 3mm. The device is filled with 0.1 -0.5 torr H_2

The raw data (streak camera recordings) of the discharge plasma during and after the current pulse show that the plasma is centered on the axis of the cathode hole and is a homogeneous glow of >15 mm in diameter, not a small diameter spark. Shown in figure 2 is a single exposure streak camera recording, taken with a 485.5 nm ($H\beta$) interference filter. Radial plots of the electron density at different times show a similar trend to that seen in figure 2. These graphs also indicate that the main discharge plasma begins first on axis and later expands.

The electron density was calculated from the Stark width broadening /10/ of the $H\beta$ transition at FWHM. The Doppler broadening, assuming a neutral hydrogen temperature of less than 1 eV, can be neglected at densities $>10^{15}$ cm^{-3} with an error of less than 15%. Below 10^{15} cm^{-3} the results are somewhat uncertain because the measured linewidth at FWHM approaches the limit of the apparatus used for this work. The electron density during the rising part of the pulse is clearly centered around the cathode hole, with a diameter comparable to or slightly larger than that of the hole. Shortly after the maximum of the current pulse, the electron density reaches its maximum of ≈$3 \cdot 10^{15}$ cm^{-3}, the diameter (at FWHM) of ≈17.4 mm

being reasonably close to the outer diameter of the area of the cathode surface that shows etching by the plasma-surface interaction.

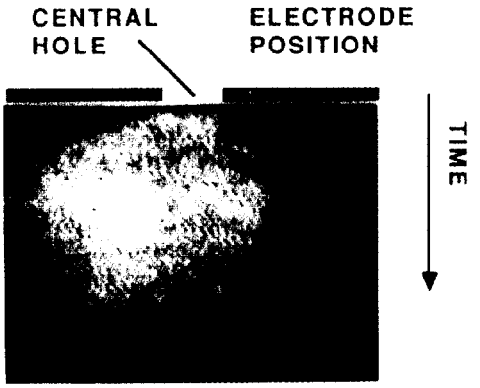

Figure 2. Streak camera photograph showing the discharge beginning near the central hole and expanding into a super-dense glow discharge.

The electron temperature was calculated from the intensity ratios of the H_α/H_β transitions for different times and radii after Abel inversion of the raw streak data. Two different models were used for computation of the temperature:

--- an LTE plasma, assuming the quantum levels $n \geq 3$ to be in (partial) equilibrium /11/

--- a partially transparent plasma, optically thin for all transitions except the Lyman series lines which are completely reabsorbed due to the large cross section for the reabsorption process. /12/

The partially transparent plasma model is a collisional radiative model relevant for a non-equilibrium, steady state hydrogen plasma of reasonable ionization and dissociation degree. Although the discharge in our plasma is not in steady state, we found that the T_e data based on the collisional radiative model of Kunc displayed the same qualitative spatial and temporal behavior as the LTE model data. There are large uncertainties in the temperature for the collisional radiative model due to the weak dependence of the line intensity ratio on temperature at $T_e > 1$ eV. Since there is evidence for a rather high ionization degree, it is reasonable to believe that the electrons dominate the collisional processes of these optically thin transitions. However, the high current density on the axis of the discharge suggests that the electron distribution function is non-Maxwellian. This is seen by a simple calculation of current density ($j \approx n_e e v_d$, where v_d is the drift velocity) which indicates that the electrons may have a drift velocity that is comparable to the thermal velocity. Thus it is likely that there is a decidedly non-Maxwellian component in the tail of the distribution function. This component, originating in the cathode region, has "beam" properties and may be a significant part of the conduction mechanism. Further work is underway to investigate this phenomena. Because the plasma may have a significantly non-Maxwellian energy distribution, determination of the electron temperature requires methods other than those employed here. Therefore, the electron temperature is undetermined for this type of discharge.

The total discharge current was measured with a current viewing resistor of 1.013 milli-ohms; the peak current at time $t \approx 250$ nsec is ≈ 8 kA. With the assumption that the conducting part of the discharge coincides with the dense, hot part of the plasma, we conclude that the lower current density limit during the main part of the current pulse is $\approx (5\text{-}10)$ kA/cm^2. This extremely high current density from an initially cold cathode of pure molybdenum is unusual and should be compared with the maximum current densities achieved with hot dispenser cathodes in thyratrons, which yield emissivities on the order of 100 A/cm^2. In the following , we discuss mechanisms leading to the increased cathode emission responsible for these high current densities.

CURRENT DENSITY

Several processes must be considered to explain the current density observed in the experiments described above. Firstly, current balance is required at the surface of the cathode, which means that the sum of electron current from the cathode plus ion current onto the cathode surface must be equal to the total discharge current at any time. Secondly, the emissivity of the cathode must be high enough to act as an electron source capable of supporting the discharge current, if electrons dominate the current in the cathode fall. In this case, different electron emission processes can contribute to the total cathode emission. These include 1) photoelectrons due to incident UV photons, 2) release of electrons due to impact of atoms (neutrals and metastables) and ions, 3) thermionic emission (eventually field-enhanced) from a heated surface layer, and 4) field emission in the presence of a high electric field at the cathode surface. Thirdly, the limitation in current density for the electron and ion flow in the cathode fall region due to their own space-charge sets an upper limit.

SPACE CHARGE LIMITED CURRENT

The space-charge limitation of electron and ion flow /13/ occurs in the cathode fall region where the mean free path of single particles is large compared to the cathode fall width and collisions can therefore be neglected. Under the assumption that the electron current is not limited by the source (e.g. the limited cathode surface emissivity), the current density is given (in esu) by /13/:

$$j_0 = \frac{1}{9\pi}\sqrt{\frac{2\cdot e}{m_e}}\,\frac{U^{3/2}}{d^2}$$

where m_e is the mass of the electron, e is the electron charge, U is the cathode fall voltage drop, and d is the electrode spacing in cm. Since the bulk plasma is essentially field free, the voltage drop is applied across the cathode fall sheath and therefore d≈width of the cathode fall). In the case of simultaneous ion flow from the anode (or, in our case, from the plasma facing the cathode) to the cathode, the electron space charge is partially canceled by the ion space charge which leads to an increase of the total current density by a factor of ≈1.86 /13/.

The maximum (space-charge limited) electron current density which can be drawn from the cathode surface assuming a voltage of 100v and $d=10^{-4}$cm is

$$j_e \approx 1.23\cdot 10^6 \ [\mathrm{A/cm^2}]$$

which is larger than the observed current density. This implies that there will be no limitation to the current density due to the space-charge limitation of charge carrier flow within the cathode fall. The ion current j_{ia} entering the cathode sheath from the anode side can be written as

$$j_{ia} = \frac{1}{2}\, e\, n_i \cdot \sqrt{\frac{2\,kT_i}{m_i}}$$

which is the maximum (saturation) ion current that can be drawn from the plasma with a stationary plasma boundary. n_i, T_i and m_i are the ion density, temperature and mass, respectively, at the plasma boundary. In our case, this yields an upper limit for the ion current density of ≈110 A/cm^2 which is much less (≈ two orders of magnitude) than the total discharge current density. This estimate requires that the electron emission capability of the cathode for the different electron release processes at the cathode surface be investigated. These include the photoelectric effect, field enhanced

thermionic emission, field emission, and secondary emission due to the impact of atoms (neutrals and excited states) and ions.

CATHODE EMISSION

The temperature of the cathode during these experiments is essentially room temperature, which is a "cold" cathode compared to typical heated thermionic cathodes of ≈1,000 K. However, during the transition phase when the current rises and the plasma builds up, prior to the "steady state" of the conduction phase, some of the loss processes involved (particle impact on the walls, radiation, etc.) can lead to a noticeable energy deposition on the walls. This energy deposition can in turn significantly heat a thin surface layer of the cathode during the current pulse. The resulting hot surface layer can act as a thermionic cathode during the pulse.

After about 10^5 pulses in hydrogen at a pressure of 27 Pa, the switch was disassembled and the cathode surface facing the anode was investigated by means of a SEM. Figure 3 shows the Mo surface near the middle of the rounded edge of the cathode hole. It is quite obvious from the cracks in the surface that the surface has been melted, probably to a depth of several micrometers, within a very short time inter- val, subsequently undergoing a very rapid quenching due to heat conduction into the cold bulk material of the cathode. From the melting point of molybdenum (2,893 K) we conclude that the surface temperature, up to a radius of ~8-9 mm, must have been close to or even above 3,000 K. This outer limit of the melting zone coincides very well with the radius (HWHM) of the plasma column as derived from the streak camera measurements. There is no evidence for melting of the cathode surface at radii r = 11 mm or larger.

Similar results have been achieved with the nickel cathode, although there are hints of surface melting up to an outer radius of ~11 mm. However, on the nickel surface no cracks appear, which may be correlated with the high ductility of Ni and the fact that, if the surface has been heated to the same temperature as the Mo electrode, the molten phase of the Ni electrode surface lasts longer and extends deeper than in the case of the Mo cathode. (The thermal properties of Ni and Mo are comparable for short-range, short-duration heat conduction.) Therefore, the Ni surface appears much smoother in the central part of the electrode.

Although the cathode surfaces appear relatively rough, showing structures which could be related to local melting (i.e. arcing), the comparatively large and smooth structures in the direct vicinity of the hole imply that much larger parts of the surface have been melted at the same time. This assumption seems to be confirmed by the fact that the cracks in the surface of the molybdenum electrode run through **all** surface structures for lengths of several 10 micrometers. We therefore assume that large parts, if not the whole cathode surface area involved (~0.4-1 cm^2), have been melted more or less evenly during single discharges.

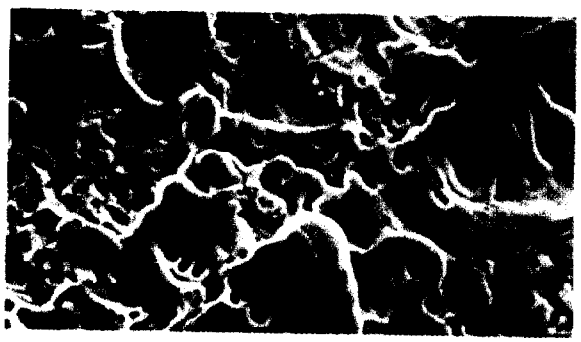

Figure 3. Scanning electron micrograph of the cathode surface at 5800x magnification. The smooth surface is evidence of melting while the cracks indicate rapid cooling.

The surface power density necessary to heat a Mo or Ni surface to a temperature of nearly 3,000 K is between 25 and 10 MW/cm^2, assuming a constant power flux of between ~30-100 nsec in duration. The only possible source of energy for this process is an intense ion current, produced in the cathode fall during the initial part of the discharge. The high temperature of up to 3,000 K is achieved over a comparably large surface of the order of cm^2, in addition to the hot surface layer there will be a high field ~10^8V/m in the plasma sheath at the surface of the cathode, this combination of high temperature and field is sufficient to produce a field enhanced thermionic emission /14,15/ on the order of the observed current density.

CONCLUSION

Other processes that may contribute to the cathode emission have been estimated /16/ and all give a considerably lower emission hence we believe that field enhanced thermionic emission is the dominant emission mechanism and that the device utilizes a self heated thermionic cathode to produce the high emission observed. A further study of the heating mechanism is required to address questions of optimization of the heating mechanism and on the length of time that the high temperature can be maintained after the initial heating. Also a study of the electron distribution function in the bulk plasma is necessary to understand the conduction of the high current density .

This work was supported by ARO, AFOSR, NSF and The Deutsche Forschungemeinschaft.

REFERENCES

1. J. Christiansen and C. Schultheiss, Z. Physik A **290**, 35 (1979).
2. D. Bloess, et al, Nucl. Instr. Meth. **205**, 173 (1983).
3. G. Mechtersheimer, R. Kohler, T. Lasser, and R. Meyer, J. Phys. **E 19**,466 (1985).
4. K. Frank et al, in press, IEEE Trans. on Plasma Sci.
5. G. F. Kirkman and M. A. Gundersen, Appl. Phys. Lett. **49** (9), 494 (1986).
6. G. F. Kirkman, W. Hartmann and M. A. Gundersen, Appl. Phys. Lett. **52** (8),613 (1988).
7. C. Braun, W. Hartmann, V. Dominic, G. F. Kirkman, M. A. Gundersen and G. McDuff, IEEE Transact. El. Dev. **35** (4), 559 (1988).
8. L. Yu. Abramovich, B. N. Klyarfel'd and Yu. N. Nastich, Sov. Physics - Tech. Physics **11** (4), 528 (1966).
9. G. I. Nosov and S. A. Smirnov, Instrum. & Exp. Tech. **20** (4), 1147 (1977).
10. H. R. Griem, *Spectral Line Broadening by Plasmas,* Academic Press, N. Y. (1974).
11. G. Bekefi, *Principles of Laser Plasmas,* Wiley, N. Y. (1976).
12. J. A. Kunc, S. Guha, and M. A. Gundersen, Lasers and Particle Beams,**1** (4), 395, (1983). See also D. A. Erwin, J. A. Kunc, and M. A. Gundersen Appl. Phys. Lett. **48** (25), 1727 (1986) and references therein.
13. I. Langmuir, Phys. Rev. **2**, 450 (1913), and Phys. Rev. **33** (6), 954 (1929).
14. W. Schottky, Z. Physik **14** (4), 63 (1923).
15. E. L. Murphy and R. H. Good, Phys. Rev. **102** (6), 1464 (1956).
16. W. Hartmann, V. Dominic, G. Kirkman, and M. A. Gundersen, to be published.